World Academy of Science, Engineering and Technology
International Journal of Civil and Environmental Engineering
Vol:9, No:3, 2015

Nonlinear Finite Element Modeling of Unbonded Steel Reinforced Concrete Beams

Fares Jnaid, Riyad Aboutaha

***Abstract*—**In this paper, a nonlinear Finite Element Analysis (FEA) was carried out using ANSYS software to build a model able of predicting the behavior of Reinforced Concrete (RC) beams with unbonded reinforcement. The FEA model was compared to existing experimental data by other researchers. The existing experimental data consisted of 16 beams that varied from structurally sound beams to beams with unbonded reinforcement with different unbonded lengths and reinforcement ratios. The model was able to predict the ultimate flexural strength, load-deflection curve, and crack pattern of concrete beams with unbonded reinforcement. It was concluded that when the when the unbonded length is less than 45% of the span, there will be no decrease in the ultimate flexural strength due to the loss of bond between the steel reinforcement and the surrounding concrete regardless of the reinforcement ratio. Moreover, when the reinforcement ratio is relatively low, there will be no decrease in ultimate flexural strength regardless of the length of unbond.

***Keywords*—**FEA, ANSYS, Unbond, Strain.

I. Introduction

STEEL reinforced concrete is a composite material, consisting of steel and concrete. These two materials have different mechanical properties; importantly, the tensile strength of steel is much higher than that of concrete. The loads are usually applied to the concrete and in order to transfer the stresses from the concrete to the embedded steel, a complete bond between the two materials must be secured. However, when there is a loss of bond between the two materials, the code equations for ultimate moment capacity, which are derived based on strain compatibility at all sections, become invalid [1].

When corrosion occurs, rust builds up around the reinforcement creating a volume 12 times greater than the volume of the original reinforcement. This increase in volume creates tensile stresses in the concrete surrounding the steel reinforcement. When these tensile stresses exceed the tensile strength of concrete, the concrete cracks. The cracking of concrete deteriorates the bond between steel and concrete, which in turn affects the ultimate strength and serviceability of the reinforced concrete members. Moreover, severe corrosion will cause spalling of concrete cover which also causes loss of bond between steel and concrete.

F. Jnaid, PhD, P. E. is with the SDR Engineering Consultant, 9035 Bluebonnet Blvd, Baton Rouge, LA 70809 USA (phone: 305-456-9871; fax: 214-741-3976; e-mail: fjnaid@sdrengineering.com).

R. S. Aboutaha is an Associate Professor, Dept. of Civil and Environmental Eng., Syracuse Univ., Syracuse, NY 13244 (e-mail: rsabouta@syr.edu).

A. Experimental Studies

Minkarah and Ringo [2] investigated deteriorated reinforced concrete beams with partially exposed (unbonded) tensile reinforcement, having reinforcement ratio of 0.95% and a 2,900 mm (114.17 in.) span. The study revealed that beams with over 60% exposed bar length experienced about 20% reduction in flexural strength. However, for beams with exposed reinforcement up to only 20% of total beam length, the ultimate flexural strength did not decrease significantly.

Smith and Wood [3] in turn carried out a study on 38 small-scale simply supported beams under a single-point load at different locations along the length of the beam. The unbonded length varied in different beams, and tended to be located in high shear regions. It was concluded that the increase of the unbonded length is accompanied by a decrease in flexural strength. They also indicated that the location of the applied load has a greater impact on the ultimate strength than does the length of the unbonded zone.

Carins and Zhao [4] provided a detailed study of changes in the flexural behavior of steel reinforced concrete beams with unbonded reinforcement based on the principles of equilibrium forces and strain compatibility. They tested 19 reinforced concrete beams with a total length of 3500 mm (137.79 in.). The variables that were included in the test were the reinforcement ratio, the effective depth, and the exposed length of the reinforcement. Beams were cast with different bar lengths exposed over a proportion of the span. For a beam with 1.5% tensile reinforcement, exposed over 90% of the span, a 50% loss of load-carrying capacity was reported. On the other hand, and for a beam with 0.5% tensile reinforcement exposed over 90% of the span, there was no loss of strength reported.

Raoof and Lin [5] tested a total of 44 small-scale beams, and 88 large-scale beams. They concluded that the ultimate strength decreased significantly in beams with higher tensile reinforcement ratios when compared to beams with lower ratios. In addition, the presence of compressive reinforcement increased the ultimate capacity of beams with exposed reinforcement.

Sharaf and Soudki [6] tested five beams to investigate the effects of unbonded length of bar to span ratio on the behavior and ultimate strength of reinforced concrete beams. The beams cross-sections were 100 × 150 mm (3.94 × 5.91 in.) with a span of 1500 mm (59.06 in.), and a reinforcement ratio of 1.7%. The debonding between steel and concrete was created by using special plastic tubes which were sealed to the bars by means of low viscosity silicon. The largest observed flexural strength reduction in the specimens was 35%, which was for a

specimen with reinforcement unbonded over 90% of the span. The smallest strength reduction was 9%, which was for a beam with reinforcement unbonded just over 50% of the span.

B.FEA Studies

Nokhasteh [7] carried out a study on corroded beams. The beams had different unbonded length at the tensile side. The beams were subjected to flexural tests, and a two-dimensional finite element model for deteriorated beams was developed. They also used the simplified material properties to perform an algebraic formulation for the beams. They concluded that for beams with unbonded tensile bars at the shear span, the flexural cracks were fewer but wider, very few cracks were reported along the shear span, the deflections at the midspan were larger, and the load carrying capacity slightly decreased. They also pointed out that the higher the reinforcement ratio and the unbonded length, the higher the decrease in load-carrying capacity. Moreover, they noticed that unbonded beams are subjected to higher reduction in load-carrying capacity when a concentrated load is applied rather than a uniformly distributed load.

Lundgren [8]-[10] performed a finite element analysis using software DIANA to perform corrosion cracking and pullout tests. The model accounts for bond mechanism between steel and concrete due to corrosion. They suggested that the model could simulate the bond-slip behavior of beams with ribbed or smooth bars at different corrosion levels.

Xiaoming and Hongqiang [11] performed a study on beams with low level of corrosion using FEA commercial software ANSYS. They also reported that when corrosion rate is 4% to 7%, there is a dramatic decrease in load carrying capacity.

II. FEA Model

In order to simulate the behavior of beams unbonded reinforcement, the author used the commercial finite element software ANSYS [12] to develop a finite element model; and the results were verified with experimental data by others. After being verified against experimental data, the FEA model was employed to investigate a total of 27 reinforced concrete beams with reinforcement ratios and different unbonded lengths.

A.Element Types

1.Concrete Elements

In order to model a concrete beam in ANSYS [12], a 3-D SOLID65 Element was adopted. This solid element has the capability of crushing in compression and cracking under tension. In addition, it incorporates steel rebars, which makes it ideal for reinforced concrete modeling. The solid element is defined by eight nodes, each of these nodes have three degrees of freedom; translations in the nodal x, y, and z directions as shown in Fig. 1. The element allows the treatment of nonlinear material properties. The concrete is capable of cracking (in three orthogonal directions), crushing, plastic deformation, and creep [12].

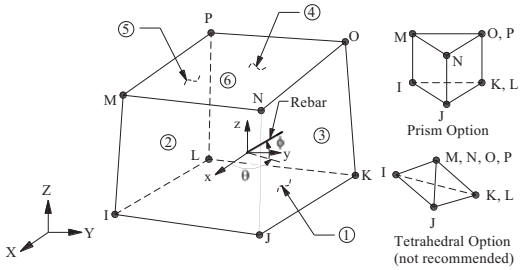

Fig. 1 SOLID65 Geometry [12]

2.Steel Elements

Steel reinforcing bars were modeled using a 3-D element LINK180. The element is a uniaxial spar capable of carrying tension and compression. The element is defined by two nodes with three degrees of freedom at each node: translations in the nodal x, y, and z directions as shown in Fig. 2. The element X-axis is oriented along the length of the element from node I toward node J. The element does not allow bending. In addition, plasticity, creep, rotation, large deflection, and large strain capabilities are considered [12].

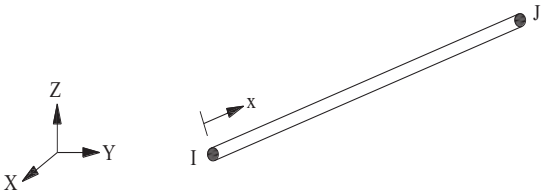

Fig. 2 LINK180 Geometry [12]

3.Spring Elements

Loss of bond between reinforcing steel and surrounding concrete was modeled using vertical spring elements COMBIN14 as shown in Fig. 3. This element has longitudinal or torsional capability in 1-D, 2-D, or 3-D applications. However, when the longitudinal spring-damper option is activated, the element is considered as a uniaxial tension-compression element with up to three degrees of freedom at each node: translations in the nodal x, y, and z directions. The element has no mass and the spring or the damper capability can be deactivated [12].

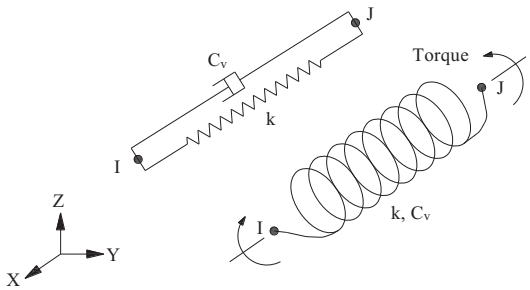

Fig. 3 COMBIN14 Geometry [12]

B.Material Properties and Real Constants

1.Concrete Elements

Von Mises failure criterion was used to define concrete failure along with William and Warnke's [13] constitutive model. The modified Hognestad stress-strain relationship was adopted to define the multilinear isotropic concrete stress-strain curves required by ANSYS, as shown in Fig. 4 (a). The stress-strain curve plotted in Fig. 4 (a) consists of 9 points, the first point is defined as $0.30f'_c$ and it represents the linear branch that satisfies Hook's law [14] and [15]. The next six points until ε_0 are calculated based on the equation describing the non-elastic branch of the modified Hognestad stress-strain relationship. The last two points represent the linear branch of the modified Hognestad stress-strain relationship. The linear branch of the curve was considered perfectly plastic since the latest versions of ANSYS [12] do not tolerate negative slopes in stress-strain plots.

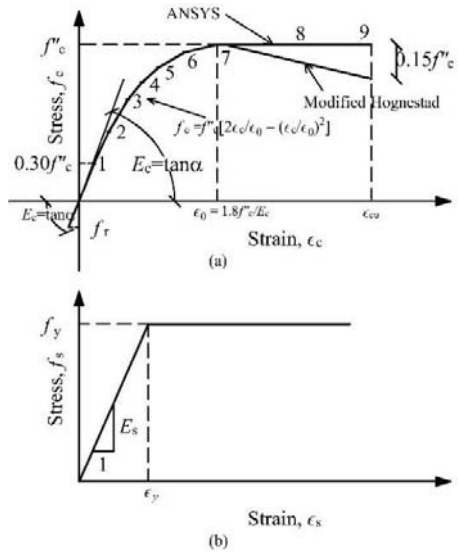

Fig. 4 Stress-strain diagrams: (a) concrete: modified Hognestad; (b) steel

The modulus of elasticity of concrete was 4,750 times the square root of concrete cube strength, uniaxial cracking stress (modulus of rupture) was 8.5% of the compressive strength, and Poisson's ratio was assumed to be 0.2. ANSYS [12] assumes a linear stress-strain relationship for concrete in tension until the uniaxial cracking stress is reached. Shear transfer coefficients range from 0 to 1, with 0 representing smooth crack (complete loss of shear transfer) and 1.0 representing a rough crack (no loss of shear transfer) (ANSYS 13.0). Shear transfer coefficient for an open crack was considered to be 0.3, and the shear transfer coefficient for a closed crack was considered to be 1 [14]-[16]. The uniaxial cracking stress and the uniaxial crushing stress were assumed to be the modulus of rupture and the concrete compressive strength respectively. The biaxial crushing stress, hydrostatic pressure, hydro biax crush stress, hydro uniax crush stress, and tensile crack factor were set equal to zero, which are their default values determined by ANSYS. These values of the above coefficients were verified by a preliminary analysis performed by the author to the best agreement with experimental data.

2.Steel Elements

An elasto-plastic stress-strain relationship was considered for steel as shown in Fig. 4 (b). The modulus of elasticity of steel was considered to be 200,000 MPa, and Poisson's ratio was assumed to be 0.3. The steel yield stress varied based on each experiment. The real constant R1, which represents the cross-sectional area of the reinforcement bars, also varied based on each experiment.

3.Spring Elements

Spring elements COMBIN14 were used to model the loss of bond. KEYOPT(1) was set to zero to activate a linear solution, while KEYOPT(2) was set to 2 in order to allow the spring to behave as a longitudinal spring-damper with a vertical UY degree of freedom. The spring stiffness was set to 100,000 N/mm. Damping coefficients and initial force were set to zero.

C.Loading and Boundary Conditions

Due to symmetry, only half of each beam was modeled in order to save computational time and to allow for a higher number of elements, the latter allowing the model to generate more accurate results. In order to model symmetry, a vertical plane (YZ) passes through the centre of the beam. The nodes defined by this plane of symmetry are constrained in the X direction, in other words, these nodes have one degree of freedom constrain UX = 0. To model the roller supports, a line of nodes on the Z axis was constrained in the Y and Z directions (UY = UZ = 0). This allows translation along the X axis and rotation about the Z. The load was applied on a line of nodes in the Z direction, the load on each node is equal to the applied load divided by the number of the nodes on the same line in the Z direction. The load was applied gradually with smaller steps at regions where the concrete starts to crack and the steel starts to yield.

D.Creating the Model

Most researchers model concrete beams by creating volumes and dividing these volumes into smaller elements by using the FE mesh command. In this research, one SOLID65 cuboid concrete element was created and then the rest of the elements were generated by copying this element along the three axes. This allows the user to change the dimensions of the whole beam by changing the dimensions of one element, and provides flexibility to use different element sizes in different locations. Flexural and shear steel reinforcement were created by attaching LINK180 steel to the concrete nodes at places where reinforcement exists. Loss of bond between reinforcing steel and surrounding concrete was modeled using vertical spring elements Combin14 with longitudinal capacity. The spring element was modeled dimensionless where steel and concrete nodes are considered to be coincident. In regions where there is perfect bond between reinforcing bars and surrounding concrete, both concrete and steel elements shared the same node. However, in the unbonded regions, identical

nodes were created at the same locations where concrete nodes existed. The two coincident nodes were connected to each other by a vertical spring with high stiffness. In order to provide a better understanding of the creation of the FEA model, the geometry of one of the beams analyzed with ANSYS is shown in Fig. 5.

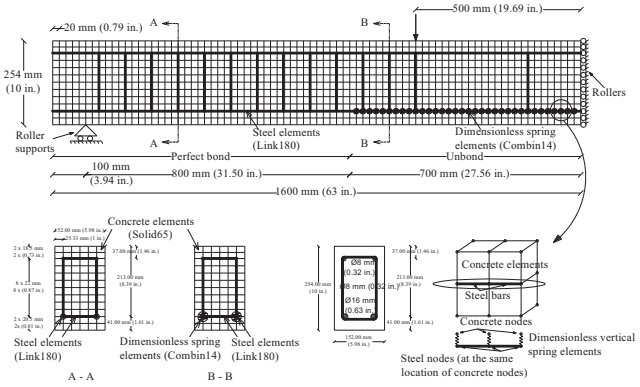

Fig. 5 Geometry of one of the beams analyzed using ANSYS [17]

E. Validation of the FEA Model

1. Validation against Cairns and Zhao [4]

Cairns and Zhao [4] tested 19 reinforced beams with exposed reinforcement, of which 11 had a rectangular cross-section and failed in flexural, i.e., concrete crushing within constant moment zone.

Due to the unavailability of load-deflection plots for the beams tested by [4], the author was not able to compare moment-deflection curves obtained by the FEA model to the experimental data obtained by [4]; however, moment-deflection curves obtained by the FEA model of beams S2, S4B, S9, and S11, tested by [4], are plotted in Fig. 6. Although beams S2 and S9 have almost the same L/d and L_{ub}/L, beam S9 was able to maintain its original capacity because of the small reinforcement ratio, which allowed the steel to yield in the tension zone. In addition, for the same reason mentioned above, beam S11 which had large L/d and relatively small L_{ub}, reached the ultimate capacity of a full bonded beam with the same length and cross-section. On the other hand, beams S2 and S4B lost 13% and 28% of their original capacity (respectively) due to the high reinforcement ratio that prevented the steel from yielding [17].

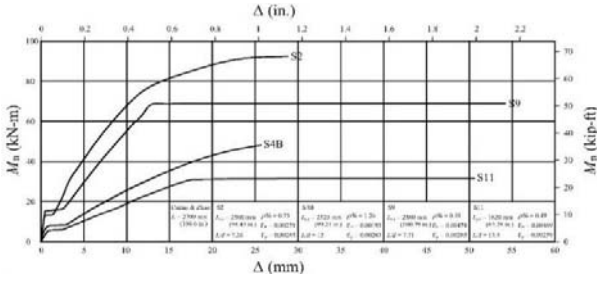

Fig. 6 Moment-deflection curves of Cairns and Zhao [4] S2, S4B, S9, and S11 (FEA)

Furthermore, the FEA model was able to predict the behavior of the beam and the crack pattern and showed good agreement with the experimental test results obtained by other researchers, as shown in Fig. 7. Cairns and Zhao [4] noted wider and higher flexural cracks within the constant moment zone and absence of cracks outside the constant moment region on the tension face. Bifurcation at the tip of flexural cracks was also observed. In addition, they noted the development of tension cracks on the compressive side of the beam at the end of the exposed reinforcement. These cracks develop in beams with exposed reinforcement over a large portion of the span, because outside the constant moment zone and towards the end of the exposed reinforcement, the stress in the steel is constant over the exposed length, whereas the moment is decreasing. This leads to a reduction in the lever arm and an increase in the depth of the neutral axis which, in turn, causes a decrease in the concrete maximum compressive stress. The depth of the neutral axis keeps increasing towards the end support until it reaches a value larger than the effective depth and the full concrete section is in compression. As the moment magnitude reduces toward the end of the unbonded length, the neutral axis appears at the top surface of the beam and moves down within the effective depth of the section. In this region, the top fibers of the cross-section are in tension and the bottom fibers are in compression, Fig. 7 (a) [4]. It was observed from ANSYS [12] that the increase of unbonded length was associated with a decrease in the number of cracks, as well as an increase in the cracks' heights.

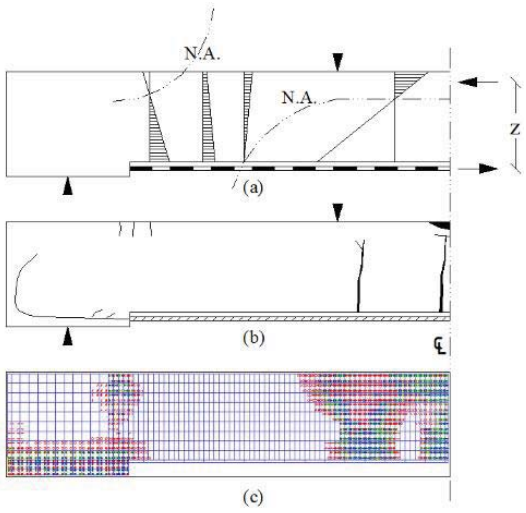

Fig. 7 Strain distribution and crack pattern of a beam with exposed reinforcement: (a) Strain distribution [4], (b) Crack pattern [4], (c) Crack pattern (FEA model)

2. Validation against [6]

Sharaf and Soudki [6] tested five beams to investigate the effects of the unbonded length of bar to span ratio on the behavior and ultimate strength of reinforced concrete beams. The beams' cross-section was 100 × 150 mm (3.94 × 5.9 in.) with a span of 1500 mm (59 in.) and a reinforcement ratio of 1.7%. The debonding between the steel and concrete was created by using special plastic tubes that were sealed to the

bars using low viscosity silicon. The specified 28-day compressive strength of concrete was 38 MPa (5.51 ksi). The specified yield strength and modulus of elasticity were 400 MPa (58 ksi) and 200,000 MPa (29,000 ksi) respectively. A comparison between the load-deflection curves obtained by [6] and the load-deflection curves obtained by the FEA model is shown in Figs. 8-12.

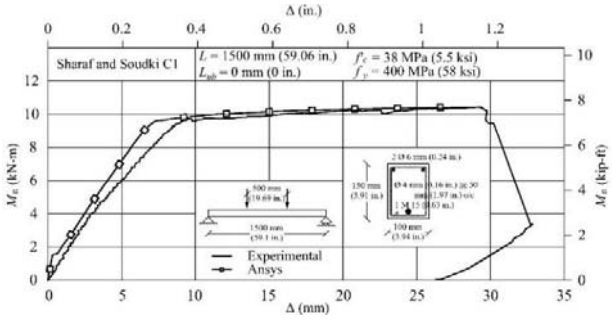

Fig. 8 Moment-deflection curve of [6] C1 (experimental vs. FEA) [17]

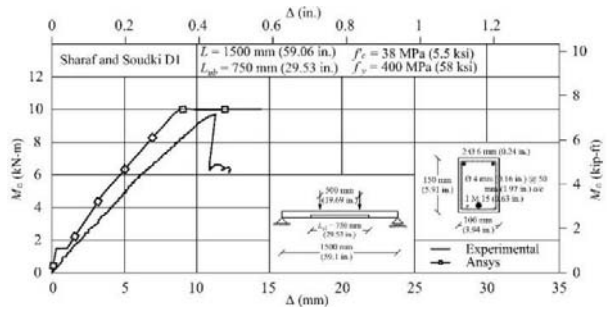

Fig. 9 Moment-deflection curve of D1 (experimental vs. FEA) [17]

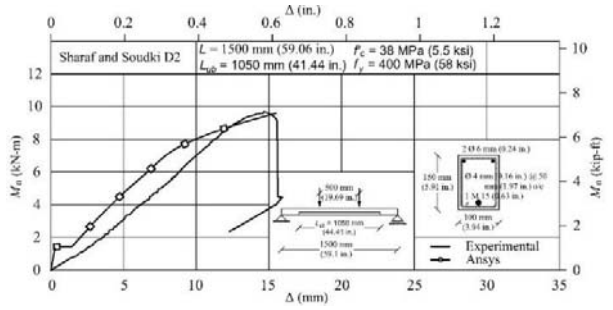

Fig. 10 Moment-deflection curve of [6] D2 (experimental vs. FEA)

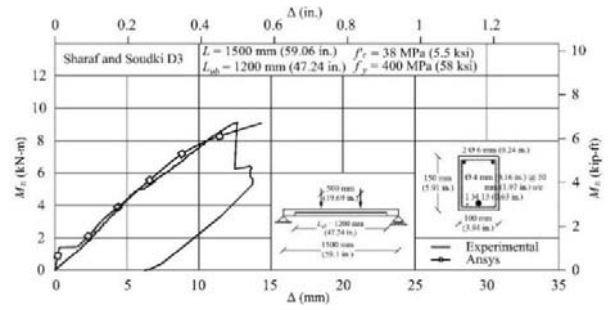

Fig. 11 Moment-deflection curve of [6] D3 (experimental vs. FEA) [17]

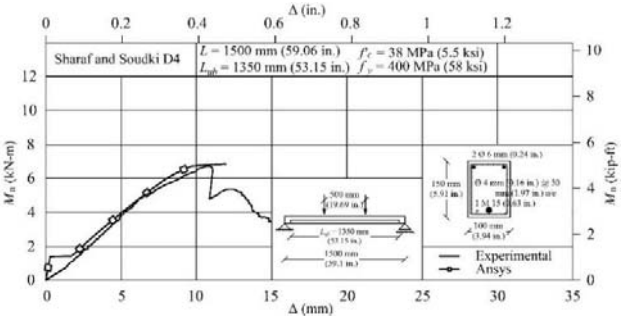

Fig. 12 Moment-deflection curve of [6] D4 (experimental vs. FEA)

It can be noted from Figs. 8-12 that the steel reinforcement in beams D2, D3, and D4 did not reach its yield strength. This is due to the reduction in strain in the steel reinforcement associated with the increase of unbonded length.

III. Comparison of FEA and Experimental Results

The FEA model was compared to 16 different experimental beams, of which one was fully bonded, and the rest were subjected to unbond between steel and surrounding concrete. The values of the ultimate flexural strength, as well as the strain at ultimate, were obtained from the FEA model and compared to the values obtained from the experimental tests by others [4] and [5]. Fig. 13 shows a comparison between the values of the ultimate strengths obtained by the experimental tests and the FEA model, while Fig. 14 shows a comparison of strain at ultimate between the FEA model and the experimental data. Note that the strain at ultimate was compared only to the experimental data obtained by [4].

It can be noted from Fig. 13 and Fig. 14 that the FEA model can reasonably estimate the ultimate capacity and strain of RC beams subjected to unbond between the reinforcement steel bars and the surrounding concrete.

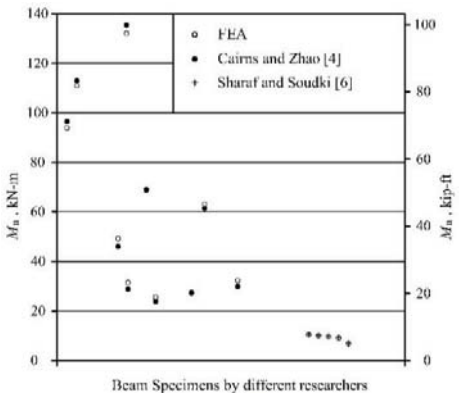

Fig. 13 Comparison of FEA with experimental results (ultimate moment)

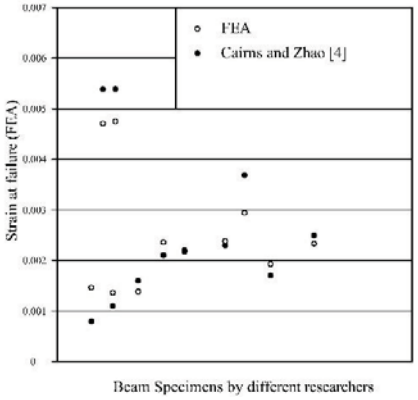

Fig. 14 Comparison of FEA with experimental results (strain at ultimate)

IV. The Effect of Reinforcement Ratio and Unbonded Length

The author employed the developed FEA to investigate the effect of reinforcement ratio on the ultimate flexural strength of beam with unbonded reinforcement. Three beams with different reinforcement ratios (0.88, 1.24, and 1.76) were investigated. ρ_{min} = 0.35, ρ_{bal} = 3.28, ρ_{max} = 2.46, and ρ_{sugg} = 1.23, where ρ_{min}, ρ_{max}, ρ_{bal}, and ρ_{msugg}, are the minimum, maximum, balanced, and suggested reinforcement ratios, respectively, as recommended by the ACI 318-11 [18]. The unbonded length varied from zero to full span. The strain in the tensile steel at ultimate in each of the cases studied was recorded and demonstrated in Figs. 15-17.

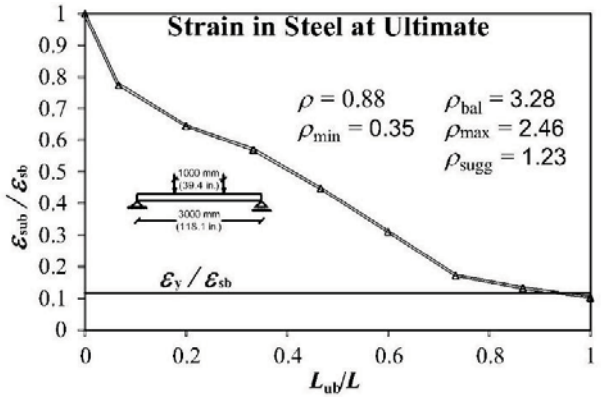

Fig. 15 Strain in beams with unbonded reinforcement (ρ=0.88)

One can conclude from Figs. 15-17 that when the reinforcement ratio is about 35% of the maximum reinforcement ratio recommended by the ACI 318-11 [18], and the unbonded length is as high as 90% of the span, the tensile steel reinforcement will reach its yield strength. In other words, there is no loss in ultimate flexural strength due to the unbond between the steel reinforcement and the surrounded concrete. With the increase in reinforcement ratio (50% of the maximum reinforcement recommended by the ACI 318-11 [18]), only beams with unbonded length that is less than 75% of the total span length were able to maintain their original flexural strength. Furthermore, when the reinforcement ratio is about 72% of the maximum reinforcement recommended by the ACI 318-11 [18], beams with unbonded length less than 45% of the span length will not experience and loss in ultimate flexural capacity due to the unbond between steel reinforcement and the surrounding concrete.

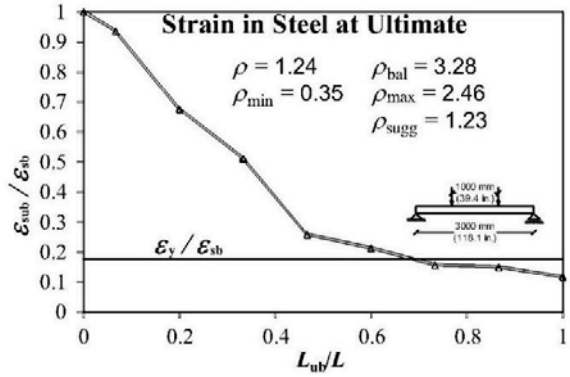

Fig. 16 Strain in beams with unbonded reinforcement (ρ= 1.24)

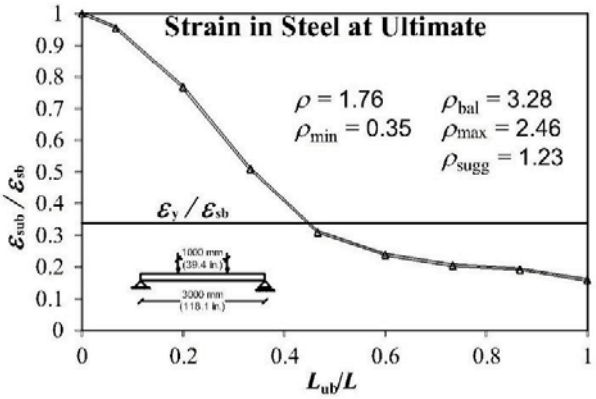

Fig. 17 Strain in beams with unbonded reinforcement (ρ= 1.76)

V. Summary and Conclusions

The commercial FEA software was employed to simulate the behavior of RC beams subjected to unbond. The loss of bond between the steel reinforcement and the surrounding concrete was modeled using vertical spring elements with high stiffness. The outcome of the FEA model was compared to 16 different beam specimens tested by others [4], [5].

It was concluded that the FEA model is able to predict the ultimate capacity and strain of RC beams subjected unbond with decent accuracy. It was also noted that the increase in unbonded length is associated with a decrease in the ultimate strength. This is because of the reduction in strain at ultimate due to unbond. However, beams with lower reinforcement ratios tend to maintain their original capacity even when the unbond between the steel reinforcement and the surrounding concrete is over a large proportion of the span. Moreover, when the reinforcement ratio is smaller than 35% of the maximum reinforcement ratio suggested by the ACI 318-11

[18], there will be no decrease in ultimate flexural strength regardless of the length of unbond.

It was also noted that beams with unbonded reinforcement develop fewer, wider, and higher cracks than beams with bonded reinforcement. This is due to the loss of bond between steel and concrete, which is responsible for crack control. The increase in the height of cracks results in a decrease in the depth of the compression zone. The height of the cracks increases whereas the number of cracks decreases with an increase of the unbonded length.

REFERENCES

[1] Eyre, J. R., and Nokhasteh, M. A. (1992). "Strength Assessment of Corrosion Damaged Reinforced Concrete Slabs and Beams." *Proceedings of the Institution of Civil Engineers, Structures and Buildings*, 94(2), 197-203.

[2] Minkarah, I., and Ringo, B. C. (1981). "Behavior and repair of deteriorated reinforced concrete beams." University of Cincinnati, Ohio, Transportation Research Record, 73-79.

[3] Smith, D. N., and Wood, L. A. (1989). "The structural performance of damaged elements," Proceedings of the International Seminar on The Life of Structures, *The Role of Physical Testing*, Brighton.

[4] Cairns, J., and Zhao, Z. (1993). "Behavior of concrete beams with exposed reinforcement." *Proceedings of the Institution of Civil Engineers: structures and Buildings*, 99(2), 141-154.

[5] Raoof, M., and Lin, Z. (1997). "Structural characteristics of RC beams with exposed main steel." *Proceedings of the Institution of Civil Engineers: structures and Buildings*, 122(1), 35-51.

[6] Sharaf, H., and Soudki, K. (2002). "Strength Assessment of Reinforced Concrete Beams with Unbonded Reinforcement and Confinement with CFRP Wraps." *4th Structural Specialty Conference of the Canadian Society for Civil Engineering*, Montreal, Quebec, Canada, 1-10.

[7] Nokhasteh, M. A., Eyre, J. R., and Mcleish, A. (1992). "The effect of reinforcement corrosion on the strength of reinforced concrete members." *Structural Integrity Assessment, P. Stanley, ed., Elsevier Applied Science*, London, England, 314–325.

[8] Lundgren, K. (2005). "Bond between ribbed bars and concrete. Part 1: Modified model." *Magazine of Concrete Research*, 57(7), 371-382.

[9] Lundgren, K. (2005). "Bond between ribbed bars and concrete. Part 2: The effect of corrosion." *Magazine of Concrete Research*, 57(7), 383-396.

[10] Lundgren, K. (2007). "Effect of corrosion on the bond between steel and concrete: an overview." *Magazine of Concrete Research*, 59(6), 447-461.

[11] Xiaoming, Y., and Hongqian, Z. (2012). "Finite Element Investigation on Load Carrying Capacity of Corroded RC Beam Based on Bond-Slip." *Jordan Journal of Civil Engineering*, 6(1), 134-146.

[12] ANSYS 13.0, "Help Manual." ANSYS, Inc., Canonsburg, Pennsylvania.

[13] Willam, K.J., and Warnke, E.P. (1974). "Constitutive Model for Triaxial Behavior of Concrete." Seminar on Concrete Structures Subjected to Triaxial Stresses, International Association of Bridge and Structural Engineering Conference, Bergamo, Italy.

[14] Kachlakev, D.I., Miller, T., Yim, S., Chansawat, K., and Potisuk, T. (2001). "Finite Element Modeling of Reinforced Concrete Structures Strengthened With FRP Laminates." California Polytechnic State University, San Luis Obispo, CA and Oregon State University, Corvallis, OR for Oregon Department of Transportation.

[15] Wolanski, A.J. (2004). "Flexural behaviour of reinforced and prestressed concrete beams using finite element analysis." M.S. thesis, Marquette University, Milwaukee, WI.

[16] Dahmani, L., Khennane, A., and Kaci, S. (2010). "Crack Identification in Reinforced Concrete Beams using Ansys Software." *Strength of Materials*, 42(2), 232-240.

[17] Jnaid, F., and Aboutaha, R. S. (2014). "Residual Flexural Strength of RC Beams with Unbonded Reinforcement," *ACI Structural Journal*, 111(6), 1419-1430.

[18] ACI 318-11 (2011). "Building Code Requirements for Structural Concrete (ACI 318-11) and Commentary." ACI 318R-11, *American Concrete Institute*, MI, USA.